The Astrophysical Journal Letters, 758:L21 (5pp), 2012 October 10 doi:10.1088/2041-8205/758/1/L21

CHARGE STATE EVOLUTION IN THE SOLAR WIND. RADIATIVE LOSSES IN FAST SOLAR WIND PLASMAS

E. Landi, J. R. Gruesbeck, S. T. Lepri, T. H. Zurbuchen, and L. A. Fisk
Department of Atmospheric, Oceanic and Space Sciences, University of Michigan, Ann Arbor, MI 48109, USA
Received 2012 July 23; accepted 2012 September 3; published 2012 September 25

ABSTRACT

We study the effects of departures from equilibrium on the radiative losses of the accelerating fast, coronal hole-associated solar wind plasma. We calculate the evolution of the ionic charge states in the solar wind with the Michigan Ionization Code and use them to determine the radiative losses along the wind trajectory. We use the velocity, electron temperature, and electron density predicted by Cranmer et al. as a benchmark case even though our approach and conclusions are more broadly valid. We compare non-equilibrium radiative losses to values calculated assuming ionization equilibrium at the local temperature, and we find that differences are smaller than 20% in the corona but reach a factor of three in the upper chromosphere and transition region. Non-equilibrium radiative losses are systematically larger than the equilibrium values, so that non-equilibrium wind plasma radiates more efficiently in the transition region. Comparing the magnitude of the dominant energy terms in the Cranmer et al. model, we find that wind-induced departures from equilibrium are of the same magnitude as the differences between radiative losses and conduction in the energy equation. We investigate which ions are most responsible for such effects, finding that carbon and oxygen are the main source of departures from equilibrium. We conclude that non-equilibrium effects on the wind energy equation are significant and recommend that they are included in theoretical models of the solar wind, at least for carbon and oxygen.

Key words: solar wind – Sun: UV radiation

Online-only material: color figures

1. INTRODUCTION

Theoretical models of the solar wind require the solution of a set of equations specifying the conservation of mass, momentum, and energy in the solar wind plasma. MHD models also add the equations that describe in detail the behavior of the magnetic field (e.g., Cranmer et al. 2007; Ofman 2010, and references therein). The energy conservation equation details the energy budget of the wind plasma; for a one-dimensional stationary model of the solar wind it takes the form (Cranmer et al. 2007)

$$u\frac{dE}{dr}+\left(\frac{E+P}{A}\right)\frac{d}{dr}(uA)=E_{\rm rad}+E_{\rm cond}+E_{\rm H}, \qquad (1)$$

where E is the internal energy density, P is the pressure, u is the bulk flow speed, and A is the cross-sectional area of the one-dimensional flux tube along which the wind flows. The left-hand-side terms of Equation (1) indicate the enthalpy transport and adiabatic cooling of the wind plasma. The right-hand-side terms $E_{\rm rad}$, $E_{\rm cond}$, and $E_{\rm H}$ describe the radiative loss, energy conduction, and heating terms, respectively. An accurate determination of the radiative losses is a fundamental ingredient to the solution of the energy equation, especially in the cases where radiation is a dominant term and determines the evolution of the plasma (see, for example, Reale & Landi 2012).

In an optically thin plasma, the energy lost to radiation per unit volume is expressed as $E_r = n_e n_{\rm H} L(T)$, where n_e and $n_{\rm H}$ are the electron density and hydrogen densities, respectively, and $L(T)$ is the plasma total emissivity, indicating the power lost to radiation per unit emission measure, in erg cm^3 s^{-1}. The term $L(T)$ is calculated using spectral codes such as the CHIANTI database (Dere et al. 1997; Landi et al. 2012b) including all relevant atomic parameters and transition rates for line and continuum emission. In almost all theoretical models of solar plasmas, $L(T)$ is calculated assuming ionization equilibrium, and it is dependent on the electron temperature only. Figure 1 shows the plasma emissivity as a function of temperature using two sets of element abundances: photospheric abundances from Grevesse & Sauval (1998) and coronal abundances from Feldman et al. (1992). While the shape of the coronal section of the radiative losses (e.g., $\log T \geqslant 5.8$) is sensitive to the element fractionation in the solar corona known as the FIP effect (Feldman & Laming 2000 and references therein), the transition region and the upper chromosphere are not. The dependence of $L(T)$ on n_e, element abundances, and ionization equilibrium data set was discussed in detail by Landi & Landini (1999), who found that (1) the electron density has limited effects on $L(T)$, (2) different choices of the ionization equilibrium data set can alter the plasma emissivity significantly, and (3) the largest source of variation is the element abundances, as shown by Figure 1.

The aim of this Letter is to show that an additional factor is able to significantly alter the plasma emissivity $L(T)$ in the accelerating solar wind: wind-induced departures from ionization equilibrium. Taking as an example the fast, coronal hole-associated solar wind, we show that such effects need to be taken into account in any theoretical model for which radiative losses have a significant effect on the solar wind. We first review in Section 2 the evolution of the charge state distribution in the fast solar wind, and discuss in Section 3 the non-equilibrium effects on radiative losses in the fast wind plasma. Section 4 summarizes the results.

2. ION ABUNDANCES IN THE ACCELERATING SOLAR WIND

Plasma acceleration and dynamics have significant effects on the charge state distribution of the nascent solar wind very close to the Sun, especially in the innermost corona where the

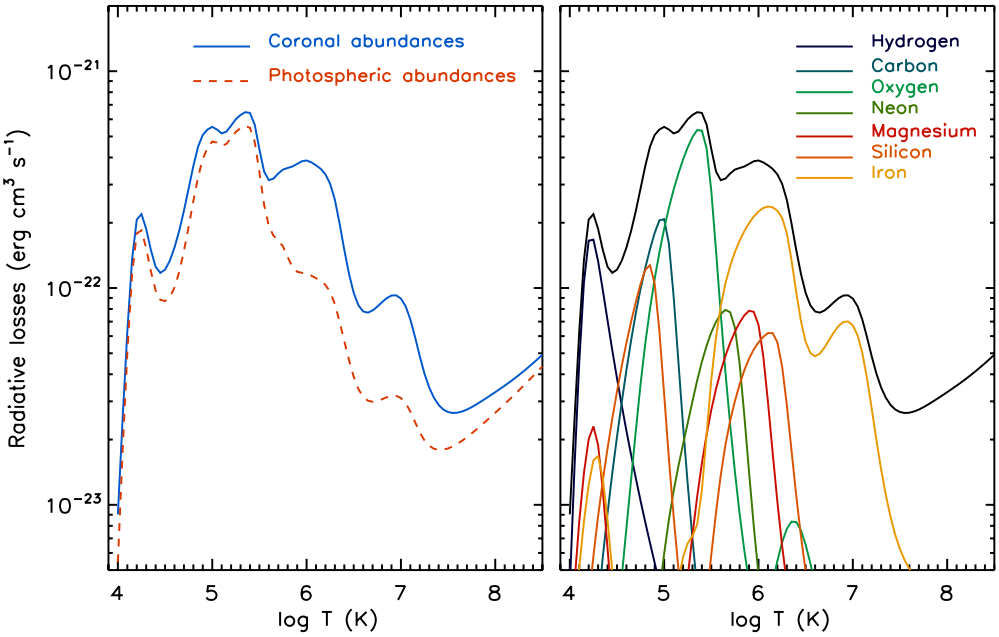

Figure 1. Radiative loss curves for a plasma with photospheric and coronal abundances, as a function of temperature. From the CHIANTI database.
(A color version of this figure is available in the online journal.)

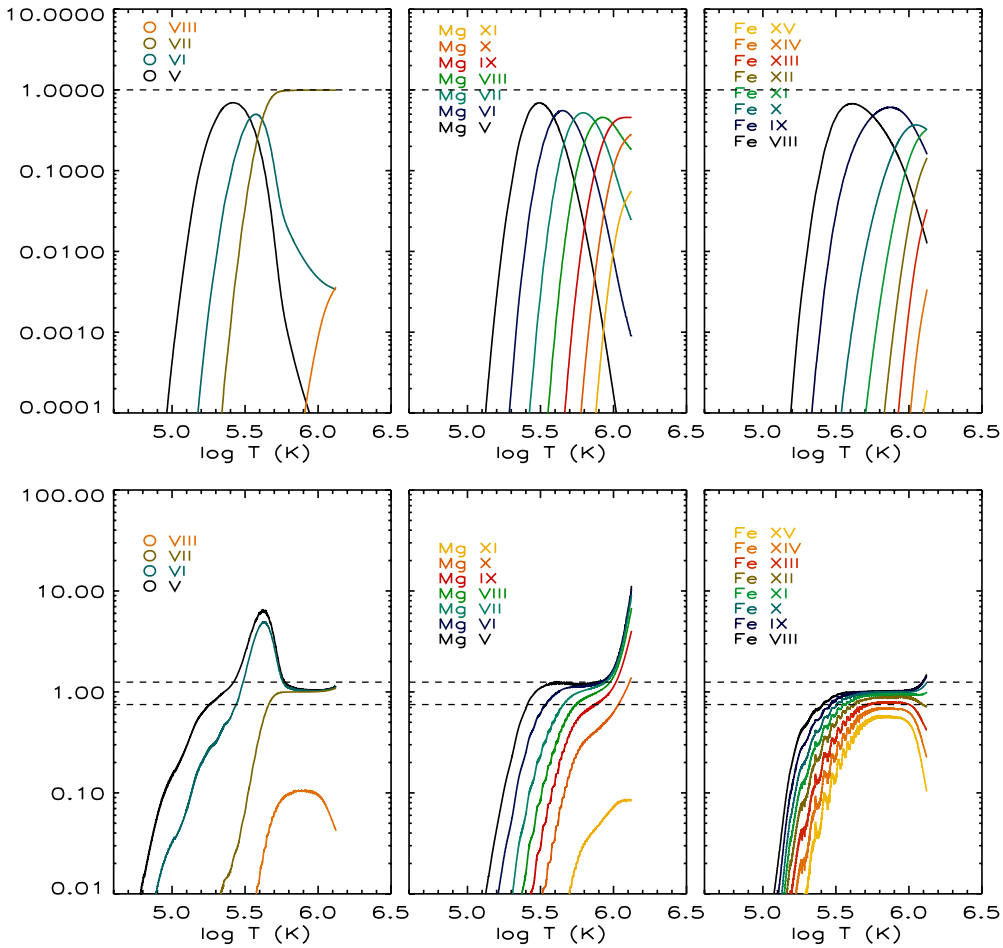

Figure 2. Charge state evolution of oxygen (left), magnesium (middle), and iron (right), as a function of temperature for heights below 1.6 R_{sun}. Top: charge state fractional abundances, from MIC (described by Gruesbeck et al. 2011; Landi et al. 2012a) and in the text. The dashed line indicates a value of unity. Bottom: ratio between the charge states calculated using MIC to ionization equilibrium values at the local temperature, to indicate the extent of departures from equilibrium. The dashed lines mark 25% from unity.

(A color version of this figure is available in the online journal.)

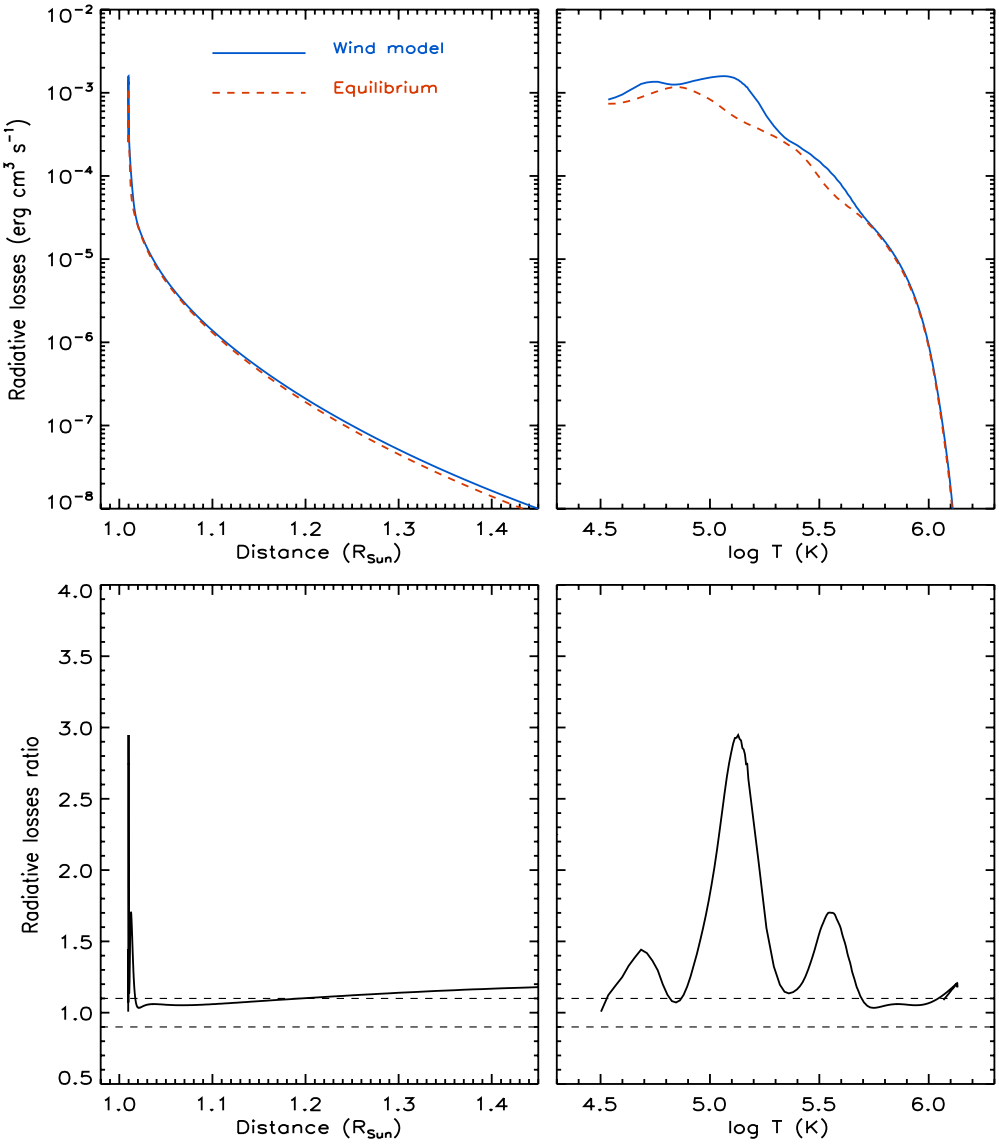

Figure 3. Top: absolute value of the radiative losses in the energy equation, as a function of distance from the limb (left) and temperature (right). Blue line: radiative losses calculated using the MIC non-equilibrium charge states; red line: values obtained assuming ionization equilibrium at the local electron temperature. Bottom: ratio of the MIC radiative losses to values calculated assuming ionization equilibrium at the local temperature, as a function of height (left) and temperature (right). The dashed line indicates a 10% departure from equilibrium.

(A color version of this figure is available in the online journal.)

density is largest and the radiative losses are most important. Such effects were investigated by Landi et al. (2012c), whose results we summarize here.

The main drivers of dynamical effects on the wind charge state distribution are the plasma density and temperature, and the ionization and recombination rates, which are directly proportional to n_e. In fact, as the wind plasma is accelerated outward from the innermost regions of the solar atmosphere (the chromosphere), it experiences a very quick decrease in electron density and a sudden increase in the electron temperature. As the wind moves through such steep gradients, its ability to ionize decreases with the density, so that the timescales for ionization (as well as recombination) lengthen, while the time spent at any given temperature shortens because of the wind's rising velocity. As a consequence, the wind charge state distribution does not have enough time to adapt to the rapidly rising local temperature and lags behind: The wind departs from equilibrium.

Landi et al. (2012c) calculated the evolution of the charge state distribution of fast wind plasma using the Michigan Ionization Code (MIC; Gruesbeck et al. 2011; Landi et al. 2012a) and the electron temperature, electron density and wind velocity profiles as a function of height predicted by the coronal hole/fast wind model by Cranmer et al. (2007). MIC solves the equations for the charge state evolution of any given element using ionization and recombination rate coefficients from CHIANTI. The charge state evolution is calculated for each element separately. For each element, an adaptive grid is selected to ensure that at any given step along the element's path the maximum variation in any of the charge states of the element is smaller than 10%. Examples of such evolution are shown in Figure 2 for three key elements: oxygen, magnesium, and iron. Figure 2 shows only the ions which emit strong lines in transition region and coronal spectra. All elements (including the most abundant ones) lose equilibrium when accelerated in the fast solar wind.

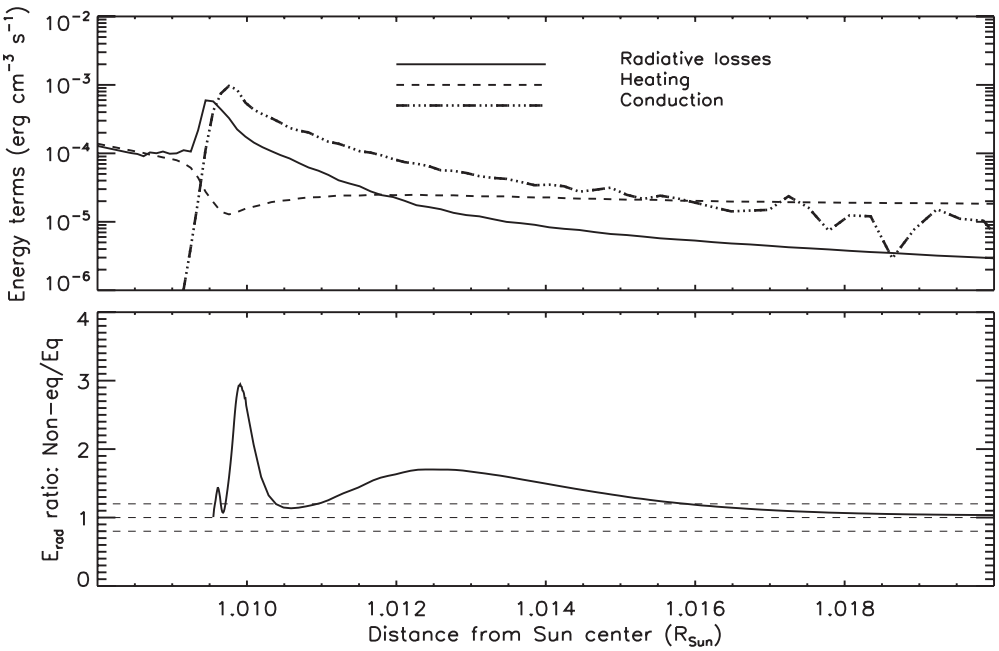

Figure 4. Top: absolute values of the main dominant terms in the energy equation of the Cranmer et al. (2007) model as a function of height in the transition region: radiative losses, conduction, and wave heating. Bottom: ratio of radiative losses calculated using MIC to values calculated assuming ionization equilibrium at the local temperature. Dashed lines indicate ±20%.

Landi et al. (2012c) identified two main effects induced by wind dynamics: the *Delay Effect* and the *Cold Effect*. The Delay Effect consists of the systematic lagging of the charge state distribution of an element behind the equilibrium distribution at the local electron temperature. The Delay Effect can be explained by looking at Figure 2 (middle), which shows the effect for magnesium. Cranmer et al. (2007) place the source region of the solar wind in the lower chromosphere, where MIC assumes ionization equilibrium as a lower boundary condition. Thus, the initial charge state distribution is shifted toward very low charge states. As the wind moves outward, the temperature increases so the charge state distribution of the element starts to shift toward higher charge states. However, as the electron density rapidly decreases, the ionization timescales increase, leading to less efficient ionization and thus to (1) overabundance of lower charge states and (2) underabundance of higher charge states relative to the equilibrium values at the local temperature. This is what all magnesium ions in Figure 2 experience; a clear example can be seen at $\log T = 6.0$, where Mg VI to IX are overabundant, while the higher stage Mg XI is largely underabundant. Overall, the magnesium charge state distribution is closer to that of a plasma with lower temperature than the actual local value, as if its charge state evolution were delayed. The Delay Effect can provide deviations of factors of 10 or more from the equilibrium values.

The ionization and recombination rates of the iron ions are much faster than those of lighter elements, so these elements are able to adapt faster to local conditions. Even though Fe ions (shown in the right panel of Figure 2) are all affected by the Delay Effect when they start to be formed at lower temperatures, they are able to adjust to coronal temperatures (which vary more smoothly than transition region temperatures) and reach ionization equilibrium in almost all cases except Fe XIII-XV, whose total ion fraction is small in coronal holes and thus do not contribute much to the wind radiative losses. Since iron dominates the radiative losses in the corona, wind-induced departures of $L(T)$ from equilibrium are expected to be small at temperatures larger than $\log T \simeq 5.8$.

The Cold Effect is a special case of the Delay Effect. Oxygen ions like O V-VII start by being delayed, and when $\log T \simeq 5.4$, O V,VI begin to be overabundant while O VII is still underabundant. However, the presence and nature of O VII changes the behavior of oxygen. In fact, O VII is a He-like ion with a noble gas electron configuration and it has very long ionization timescales that effectively almost stop this ion from being further ionized: As a consequence, its charge state fractional abundance approaches unity at $\log T \simeq 5.7$. At the same time, O VII recombination rates are of the same order of magnitude as the O V,VI ones, whereas O V,VI ionization rates are relatively fast. As a consequence, ionizations and recombinations to and from O V-VII occur approximately at the same rate and these ions seem to be in equilibrium. Thus, the O V,VI charge states are overabundant at around $\log T \simeq 5.5$–5.6 by a factor of almost 10, and then revert to equilibrium values. We refer to this spike as the Cold Effect. A similar behavior is shown by the other elements who are able to reach the He-like electron configuration: carbon and nitrogen. Therefore, the emission of ions like C III,IV and O V,VI, critical to the radiative losses in the transition region (as shown in Figure 1), is greatly enhanced. Since these two elements dominate the radiative losses at $\log T = 5.0$–5.5, large effects are expected on $L(T)$ in the transition region.

3. RADIATIVE LOSSES IN THE ACCELERATING SOLAR WIND

Figure 3 (top) shows the radiative losses calculated as a function of height and of temperature using MIC and the Cranmer et al. (2007) temperature, density, and velocity profiles. Radiative losses are largest in the regions lower than the corona, where the electron density is largest and the plasma radiates more efficiently. Also, differences in the radiative losses calculated with and without the assumption of radiative

equilibrium are largest at low temperatures, where the Cold Effect modifies the charge state distribution and the emissivity of carbon and oxygen. The ratio of the non-equilibrium radiative losses to the equilibrium values is shown in Figure 3 (bottom), as a function of distance from the limb and of temperature; the dashed lines mark a 10% difference. While the corona is affected by wind-induced departures from equilibrium by less than 20% at any height, the transition region radiative losses change by a factor up to three.

To understand whether such departures are important in the overall energy budget of the transition region, Figure 4 displays the three dominant energy terms in the energy equation of the Cranmer et al. (2007) model (kindly provided to us by Dr. S. R. Cranmer) as a function of height in the transition region. Cranmer et al. (2007) radiative losses were based on CHIANTI radiative losses calculated under the assumption of local equilibrium at $\log T > 4.0$ for all elements except hydrogen, for which the output of the PANDORA radiative transfer code (Avrett & Loeser 2003, 2008) was used; they were also extended to the photosphere taking into account radiative transfer and other effects (see Cranmer et al. 2007 for details). However, at the temperatures of interest for this comparison ($\log T > 4.5$), departures from equilibrium take place at temperatures where hydrogen emission is not dominant and radiative transfer is negligible. At the heights where the departures are largest ($\approx 1.010\ R_{\rm sun}$), wave heating is negligible and the energy equation is dominated by radiation and conduction; the latter is larger than the radiative losses but the magnitude of the difference is very similar to the magnitude of the change to the radiative losses caused by the wind-induced departures from equilibrium. On the contrary, radiative losses are negligible in the corona, where the energy equation is dominated by heating and conduction because the decrease in the electron density dramatically reduces the magnitude of the radiative losses.

4. CONCLUSIONS

Figures 3 and 4 clearly show that the effects of non-equilibrium ionization are small and are expected to have no consequence to the wind energy equation in the corona, while they may have a significant impact in the transition region. While it is unlikely that they will completely change the results of the model, nonetheless the effects of non-equilibrium may shift the location of the transition region outward, and affect the overall structure of the lower solar atmosphere. Therefore, we recommend that non-equilibrium ionization, at least for the most important elements contributing to the radiative losses in the transition region, be included explicitly in the calculation of the energy lost by the plasma through radiation. Figure 1 shows that the relevant elements in the upper-chromosphere/transition region temperature range are carbon, oxygen, and, to a lesser extent, silicon. While silicon shows small sensitivity to wind-induced departures from equilibrium in the transition region (e.g., Landi et al. 2012c), carbon and oxygen are strongly affected by the Cold Effect and thus their charge state evolution needs to be included explicitly in the energy equation.

Departures from equilibrium of all other elements can be neglected in the energy equation. However, they need to be taken into account when model predictions are used to calculate synthetic line intensities and narrow-band images for comparison with observations.

As a last remark, we note that the present results have been obtained by using the electron temperature, density, and velocity curves from the fast wind model by Cranmer et al. (2007). Since the charge state distribution is very sensitive to the particular input profiles fed into MIC, other models may be affected by departures from equilibrium in a slightly different way. We recommend that non-equilibrium effects on the radiative losses be checked in any theoretical model of the fast and slow solar wind developed assuming equilibrium radiative losses.

The work of E.L. is supported by the NNX11AC20G and NNX10AQ58G NASA grants, and by grant AGS-1154443 from NSF. J.R.G. is supported by the GRSP program through grant NNX10AM41H. T.H.Z. and S.T.L. are supported by NASA through contract NNX08AI11G and grants NNX07AB99G and NNX10AQ61G. L.A.F. is supported by NSF grant AGS-1043012. The authors warmly thank Dr. S. R. Cranmer for kindly providing the theoretical temperature, density, and velocity profiles as well as the radiative, conductive, and heating terms used in this work.

REFERENCES

Avrett, E. H., & Loeser, R. 2003, in IAU Symp. 210, Modeling of Stellar Atmospheres, ed. W. Weise & N. Piskunov (Dordrecht: Kluwer), A-21
Avrett, E. H., & Loeser, R. 2008, ApJS, 175, 229
Cranmer, S. R., van Ballegooijen, A. A., & Edgar, R. J. 2007, ApJS, 171, 520
Dere, K. P., Landi, E., Mason, H. E., Monsignori Fossi, B. C., & Young, P. R. 1997, A&AS, 125, 149
Feldman, U., & Laming, J. M. 2000, Phys. Scr., 61, 222
Feldman, U., Mandelbaum, P., Seely, J. L., Doschek, G. A., & Gursky, H. 1992, ApJS, 81, 387
Grevesse, N., & Sauval, A. J. 1998, Space Sci. Rev., 85, 161
Gruesbeck, J. R., Lepri, S. T., Zurbuchen, T. H., & Antiochos, S. K. 2011, ApJ, 730, 103
Landi, E., Alexander, R. L., Gruesbeck, J. R., et al. 2012a, ApJ, 744, 100
Landi, E., Del Zanna, G., Young, P. R., Dere, K. P., & Mason, H. E. 2012b, ApJ, 744, 99
Landi, E., Gruesbeck, J. R., Lepri, S. T., & Zurbuchen, T. H. 2012c, ApJ, submitted
Landi, E., & Landini, M. 1999, A&A, 347, 401
Ofman, L. 2010, Living Rev. Sol. Phys., 7, 4
Reale, F., & Landi, E. 2012, A&A, 543, A90